 DOI: 10.1002/masy.200650123

Polymer Nanocomposites: How to Reach Low Flammability?

Serge Bourbigot, Sophie Duquesne, Charaf Jama*

Summary: The paper investigates critically the feasibility to make fire proof polymer using nanoparticles. It includes organoclay, polyhedral oligomeric silsesquioxanes (POSS) and carbon nanotube (CNT). It is shown that they can be used to make material exhibiting low heat release rate (HRR) when they undergo heat. We have developed novel approaches to characterize quantitatively the nanodispersion by solid state NMR and by TEM associated with image analysis and we have demonstrated that the dispersion at the nanoscale is essential to achieve the best performance. On the other hand, low flammability of nanocomposites is only achieved in terms of HRR but they fail in terms of UL-94 and limiting oxygen index (LOI). To overcome this problem, we have combined nanoparticles with traditional flame retardants (intumescents) or with plasma treatment. The nanofillers act as synergists and offer an exceptional way for making fire safe polymers.

Keywords: carbon nanotubes; clay; cold plasma; flame retardancy; nanodispersion; polymer nanocomposite; POSS

Introduction

Various methods can be used to protect materials more effectively against attack by fire. An efficient way is to use flame retardants and/or particles (micro- or nanodispersed) directly incorporated in the materials (e.g. thermoplastics or thermosets) or in a coating covering their surface (e.g. structural steel or textiles) [1]. This approach is chosen in this work to provide low flammability to polymeric materials because it is an acceptable compromise between cost and properties and because it brings great flexibility to design materials with multifunctional properties.

The pioneering work of Gilman et al. has demonstrated that the presence of nanodispersed montmorillonite clay in polymeric matrices produces a substantial improvement in fire performance [2–4]. Gilman and other groups subscribed this approach and developed hybrid polymeric materials including organomodified clays [5–8], nanoparticles of TiO_2[9], nanoparticles of silica [10], layered double hydroxides (LDH) [11–12], carbon nanotubes (CNT) [13–14] or polyhedral silsesquioxanes (POSS) [15–17]. All those materials exhibit low flammability associated to other properties such as enhanced mechanical properties. Typically, peak of heat release rate (HRR) is decreased by 50 up to 70% in a cone calorimeter experiment.

The aim of this paper is to investigate the use of different nanofillers to provide flame retardancy (FR) to polymer in order to try to answer our title question ''how to reach low flammability with the ''nano'' approach?''. Three kinds of nanofillers will be considered, organomodified clays, POSS and CNT. They will be examined based on our recent results and on the literature. The aspect of dispersion (nanodispersion of the filler) will be particularly taken into account in order to examine its impact on flame

Laboratoire Procédés d'Elaboration des Revêtements Fonctionnels (PERF), UPRES EA 1040, Ecole Nationale Supérieure de Chimie de Lille (ENSCL), Avenue Dimitri Mendeleïev – Bât. C7a, BP 90108, 59652 Villeneuve d'Ascq Cedex, France

retardancy. The final part of the paper will discuss the opportunity of using nanoparticles as flame retardant and will be also devoted to the benefit of combining the ''nano'' approach with other flame retardancy concepts.

Polymer Clay Hybrid Nanocomposite

Montmorillonite (MMT) clays (mica-type layered silicates) organomodified by methyl, tallow, bis-2-hydroxyethyl, quaternary ammonium chloride (Cloisite 30B from Southern Clay Product at San Antonio, TX and hereafter called C30B) and raw MMT (Cloisite Na+ from Southern Clay Product at San Antonio, TX and hereafter called Na+) was melt blended with poly(ethylene-co-vinyl acetate) (EVA, EVA containing 19% vinyl acetate) according to a protocol described in [18]. EVA-C30B exhibits an intermediate structure exfoliated/intercalated while EVA-Na+ is a microcomposite.

Cone calorimetry experiments reveal that the peak of heat release rate (HRR) is decreased by 25% for the microcomposite (EVA-Na+) and by 50% for the nanocomposite (EVA-C30B) compared to the virgin EVA (Figure 1). This result is consistent with previous published works [5,19,20] in which it was claimed that nanodispersion permits to provide the best FR performance. Wilkie et al. [21] also suggested that no reduction or a slight reduction in HRR peak can be taken as an indication that nanocomposite formation has not occurred. A quick overview of the literature indicates that it is probably true [18–21].

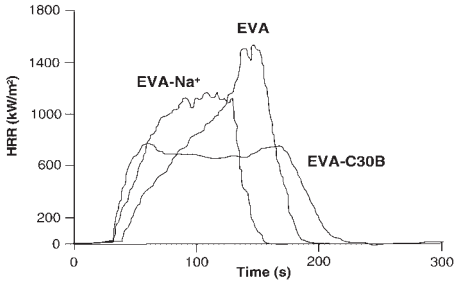

Figure 1.
Comparison of the heat release rate (HRR) plots for pure EVA, EVA-Na + (microcomposite) and EVA-C30B (nanocomposite) at 50 kW/m^2 heat flux with a mass fraction of 5% layered silicate.

Nanodispersion versus microdispersion is one of the key factor to make flame retarded polymer. If it is well accepted in the case of clay that nanodispersion should be achieved to reach good FR performance, no indication is mentioned about the role of the morphology of the nanocomposite on the FR performance. In general, polymer clay composites are of three categories [22]: (i) Microcomposites: the clay tactoids exist with no penetration of the polymer into the clay lamellae; (ii) Exfoliated composites: the individual clay layers are dispersed as single platelets into a continuous polymer matrix; (iii) Intercalated composites: in an intercalated composite the insertion of polymer into the clay structure occurs so as to swell the spacing between platelets in a regular fashion, regardless of the clay to polymer ratio. Usually, however an intercalated nanocomposite is normally interlayered by only a few molecular layers of polymer. Depending on the polymer/clay ratio, free polymer may or may not exist outside of the clay regions. From this brief description of polymer clay nanocomposites it should be evident that techniques are needed to characterize the nanocomposite with resolution at the nanoscale. Traditionally this is done using transmission electron microscopy (TEM) and X-ray diffraction (XRD) [20]. TEM and XRD provide essential information on the structure of the nanocomposite; TEM gives qualitative information and extensive imaging is required to insure a representative view of the whole material, while XRD allows quantification of changes in layered-silicate layer spacing. Those two methods do not permit to quantify the degree of nanodispersion of the layered-silicate in the bulk polymer. To overcome this we have developed at NIST a novel method using solid state nuclear magnetic resonance (NMR) of protons. It is able to quantify the degree of nanodispersion of the layered-silicate in the bulk polymer [24–25]. The

method is based on T_1^H (proton longitudinal relaxation time) measurement. The success of the method depends on two effects: 1) the paramagnetic character of the naturally occurring MMT (which directly reduces the T_1^H of nearby protons) and 2) spin diffusion, whereby this locally enhanced relaxation propagates to more distant protons [26–28]. The interpretation of those effects permitted us to extract 2 parameters relating to the dispersion. The first parameter, f, is the fraction of the potentially available clay surface which has been transformed into polymer/clay interfaces (in the NMR sense, it means that intercalated polymer is not counted as polymer/clay interface). The second parameter, ε, is a relative measure of the homogeneity of the dispersion of these actual polymer/clay interfaces. These parameters will be used in the following to characterize the morphology of the nanocomposite and to quantify the degree of nanomixing.

In order to investigate the effect of the morphology of the nanocomposite on the fire properties, Wilkie et al. synthesized different polystyrene (PS) according to a protocol described in reference [29]. Cloisite Na+ was organomodified by three different ammonium salts, namely, N,N-dimethyl-n-hexadecyl-(4-hydroxymethylbenzyl) ammonium chloride, OH16, N,N-dimethyl-n-hexadecyl- (4-vinylbenzyl) ammonium chloride, VB16, and n-hexadecyl triphenylphosphonium chloride, P16 [5]. The preparation of the VB16, OH16 and P16 nanocomposites with styrene was then accomplished by the bulk polymerization technique.

An exfoliated structure allows an intimate contact between each MMT platelet and the polymer; hence, maximal interfacial area will be exposed and f will be close to one. In the opposite case of a microcomposite structure, the dispersion of MMT platelets is comparatively poor and polymer/clay interfacial area is small (f will be close to zero). In the intermediate case (intercalated structure or mixed intercalated/exfoliated), the measured relaxation rate at the shorter times will be controlled by the nanodispersion of MMT, by the number and the size of tactoids and by the number of delaminated layers in the polymer ($0 < f < 1$). The values of the fraction of the interface polymer/clay available in PS, f, as well as the associated degrees of homogeneity of the nanomixing, ε, are given in Table 1.

The degree of homogeneity provides information about the quality of dispersion, or in other words, the distribution of microcomposite particles, tactoids and individual MMT platelets in the polymer. It falls between 39 and 69%. It means that the number and distribution of the relative number and sizes of tactoids or the distribution of individual MMT platelets can vary considerably from a sample to another sample. It gives us the information that a nanocomposite can exhibit a mixed intercalated/exfoliated structure with the presence of small tactoids having a good distribution of ''its structure'' (PS-OH16 and PS-P16), and on the contrary, a very well exfoliated sample by TEM and XRD (PS-VB16) shows a comparatively poor distribution of MMT platelets ($\varepsilon = 39\%$).

Table 1.
Fraction of the interface polymer/clay, f, available in PS and estimation of the degree of homogeneity, ε, in PS/MMT nanocomposites.

Polymer	Residue[(1)](wt.-%)	T_1^H(s)	R[(2)]	ε(%)	TEM/XRF conclusions
PS	0	26	0	-	-
PS/P16	2.3	9.31	0.46	69	Nanodispersed, Intercalated
PS/OH16	2.0	10.5	0.34	63	Nanodispersed, Intercalated/Exfoliated
PS/VB16	2.0	9.00	1.0	39	Exfoliated

(1) Residue at 800 °C measured by TGA in air;
(2) The lower f value of PS/OH16 exhibiting a mixed morphology intercalated/exfoliated regard to PS/16 exhibiting an intercalated structure suggests the presence of tactoids larger in size for PS/OH16 than for PS/P16 (see [25] for complete discussion).

PS nanocomposites containing OH16, P16 and VB16 clays have been already evaluated by cone calorimetry by oxygen consumption in a previous paper [5]. Only main conclusions are presented here. It was found that nanocomposites clays have a lower heat release rate (HRR) than does the virgin polymer (Figure 2). The peak of HRR (PHRR) of the virgin PS is 1025 kW/m^2 and those of PS-P16, PS-VB16 and PS-OH16 fall to 590 kW/m^2, 520 kW/m^2 and 500 kW/m^2 respectively. The suggested mechanism by which clay nanocomposites function involves the formation of a char that serves as a barrier to both mass and energy transport. It should also be noticed that PHRR is decreased by about 50% for the three nanocomposites as expected for nanocomposites exhibiting a reasonable dispersion.

From Figure 2, it can be seen that there is not a large difference between the three nanocomposites. According to NMR data, PS-OH16 and PS-P16 almost exhibits the same nanostructure (same f and ε) but have 90 kW/m^2 difference in PHRR. PHRR of PS-VB16 falls in an intermediate value between PS-OH16 and PS-P16 and its nanostructure is an exfoliated structure not very well distributed in the polymer ($\varepsilon = 39\%$). This observation suggests that no definitive conclusion may be given on a relationship ''morphology of nanomixing and fire performance'' without well characterizing nanodispersion in the polymer in the case of PS systems. We need now to synthesize exfoliated PS nanocomposites with a very well distribution of MMT platelets as model to determine and to quantify precisely the effect of exfoliation on fire properties. This work is in progress in our laboratory and will be published in a separate paper.

Polymer Nanoreinforced by POSS

Structure of polyhedral oligomeric silsesquioxanes (or POSS) have been first reported in 1946 [30], but it is only recently that POSS-based hybrid polymers have received increasing attention because of the unique structure of the POSS macromer, which is a well-defined cluster with an inorganic silica-like core (Si_8O_{12}) surrounded by eight organic corner groups. The nanoscopic size of POSS enables POSS segments to effectively reinforce polymer chains-segments and control chain motion at the molecular level through maximizing the surface area and chemical interactions of the nanoreinforcement with the polymer. POSS is thus a candidate to design FR polymer nanocomposite [31–33] but few papers report the use of POSS as fire retardants for polymers and textiles.

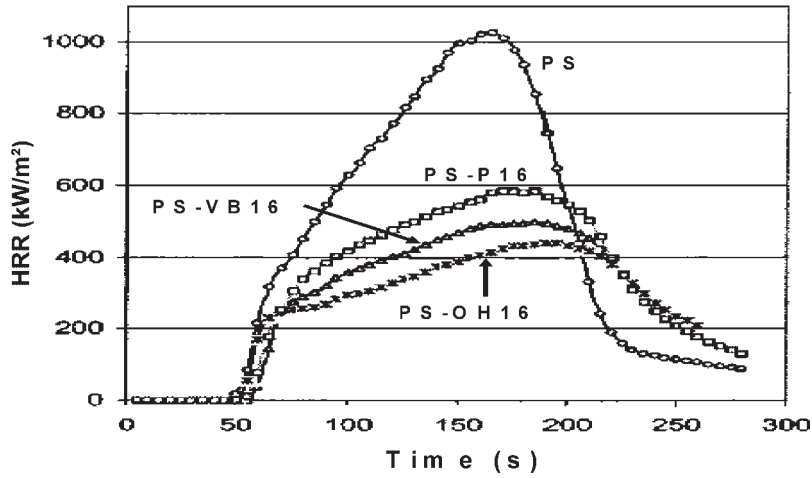

Figure 2.
Heat Release Rate (HRR) curves at 50 kW/m^2 of PS, PS-OH16, PS-VB16 and PS-P16 versus time (from [5]).

Good FR performance was achieved in polyether block amides polymer (PEBAX) making polymer reinforced by POSS. In this particular case, peak of heat release rate (external heat flux = 35 kW/m^2) of PEBAX is decreased by 77% when using POSS compared to virgin polymer (Figure 3) [34]. The suggested mechanism is char formation at the surface of the material which can act as an insulative barrier [35]. The organic groups on POSS cages undergo homolytic Si–C bond cleavage at ~300–350 °C in air. This process is immediately followed by fusion of POSS-cages to form a thermally insulating and oxidatively stable silicon-oxycarbide ''blackglass'' surface char (''Si–O–C ceramified char'') [36].

Recently, Fina et al. [37] report the use of POSS as potential fire retardant in polypropylene (PP) and polybutyleneterephthalate (PBT). The nanocomposites were prepared by melt blending and in the particular case of PBT, PHHR is decreased by 35% (external heat flux = 35 kW/m^2) compared to the virgin PBT. Concurrently, time to ignition of PBT-POSS is shorter than that of virgin (60 s *vs.* 90 s) what is a disadvantage. The authors confirm the mechanism mentioned above. They observed the formation of a ceramified char rich in silicon at the surface of the material after burning. They also suggested that this ceramic phase is responsible for the protection.

Nanocomposite textiles have not attracted much attention but in our group, we are developing this approach because we believe that we can provide substantial flame retardancy to textile alone with nanofillers or in combination with other approach (see the last section). Thermoplastic polyurethane (TPU) – nanocomposite is examined as coating for fabrics as typical example. Two kinds of POSS were used (see the chemical formulae in Figure 4 and Figure 5) and we synthesized PU-POSS nanocomposites according to the protocol described in [38].

Rate of Heat Release (RHR) curves of TPU containing POSS coated on woven polyester (PET) fabric show a significant reduction of the flammability (in terms of peak of RHR) regard to virgin TPU (Figure 6). The two POSS reveal different behaviors in TPU. The time to ignition of TPU/DP-POSS (7s) is shorter than neat TPU (10s) while that of TPU/FQ-POSS is longer (22s). The peaks of RHR of TPU/DP-POSS and TPU/FQ-POSS are decreased by 31% and by 50% respectively. During the combustion, it is observed the formation of char layer at the surface of the materials. In the case of TPU/FQ-POSS, the char is more uniform and only small

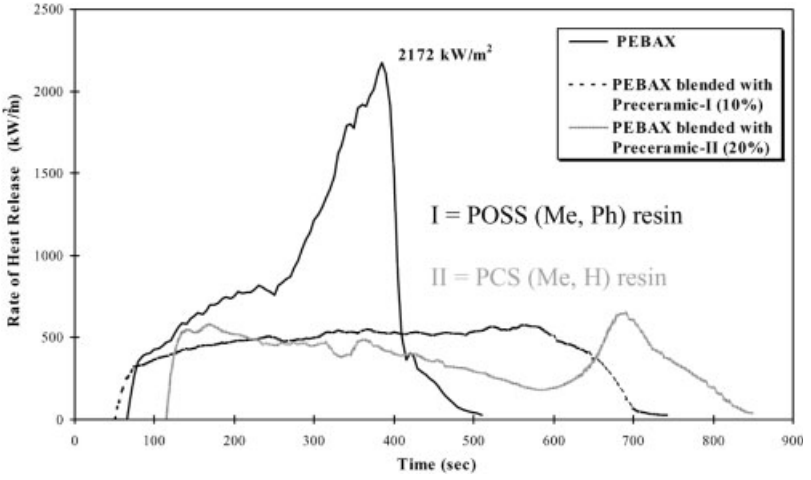

Figure 3.
Rate of Heat Release (RHR) curves versus time of PEBAX blended with POSS at 35 kW/m² (from [34]).

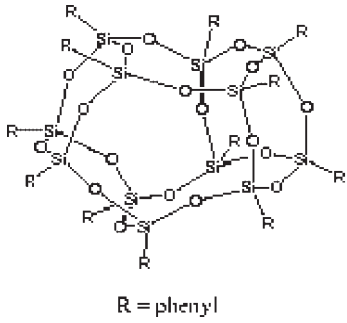

Figure 4.
dodecaphenyl-POSS (DP-POSS)

cracks are observed at the surface (cracks can be observed in the case TPU/DP-POSS which can explain its ''wavy'' curve). This char is more resistant and can smother the flame. It is also noteworthy that THE (Total Heat Evolved) of TPU/POSS (60 kJ for TPU/DP-POSS and 40 kJ for TPU/FQ-POSS) are significantly lower than neat TPU (70 kJ) showing that DP-POSS and FQ-POSS act as a real flame retardant (reaction to fire decreasing RHR and THE). We do not have investigated the mechanism of action yet but visual observation suggests that the proposed mechanism mentioned above is similar as that it occurs in the case of textile. Using POSS in TPU coating offers therefore the opportunity to make relative heat resistant fabrics. The use of FQ-POSS permits both the increase of the time of ignition and the decrease of peak of RHR. These results offer thus a promising route for flame retarding textile.

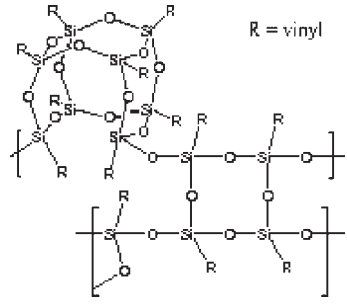

Figure 5.
poly(vinylsilsesquioxane)(FQ- POSS)

Carbon Nanotubes Dispersed in Polymer

Carbon nanotubes, the macromolecular analog of fullerenes, were found by Iijima in 1991 [39]. These are arrangements of carbon hexagons formed into tiny tubes. They may have diameters ranging from a few angstroms to tens of nanometers and can have lengths of up to several centimeters. With this type of nanoparticle, significant increases in mechanical properties and specifically in electric conductivity were reported for polymer carbon nanotube nanocomposites at low content levels of the nanotubes [40–43]. Kashiwagi et al. reported the first study on the flammability of polymer carbon nanotube nanocomposites [44]. They showed significant flame retardant effectiveness of polypropylene (PP)/multi-walled carbon nanotubes (MWNT) (1 and 2% by mass) nanocomposites. Concurrently, Beyer demonstrated a small improvement in flammability properties of ethylene-vinyl acetate (EVA)/MWNT (2.5 and 5% by mass) nanocomposites [45].

Recently, Kashiwagi et al. investigated the mechanism in which MWNT provides low flammability to PP [13]. They compared heat release rate curves of virgin PP and two PP nanocomposites containing 1 wt.-% and 2 wt.-% MWNT. The results show that the heat release rates of the PP/MWNT nanocomposites are much lower than that of virgin PP even though the amount of MWNT in PP is quite small (reduction by 80% in terms of peak of HRR). They reported that the observed FR performance of the PP/MWNT nanocomposite is mainly due to chemical and/or physical processes in the condensed phase instead of in the gas phase. The addition of MWNT in PP suppresses melting and formation of bubbles and forms MWNT network structured layer (Figure 7). The MWNT network layer shields resin from external radiation and heat feedback from flame and also acts as an excellent thermal insulation layer. Schartel et al. got similar conclusions in polyamide-6 (PA-6)/MWNT [46]. They also reported the formation of MWNT interconnected network structure during

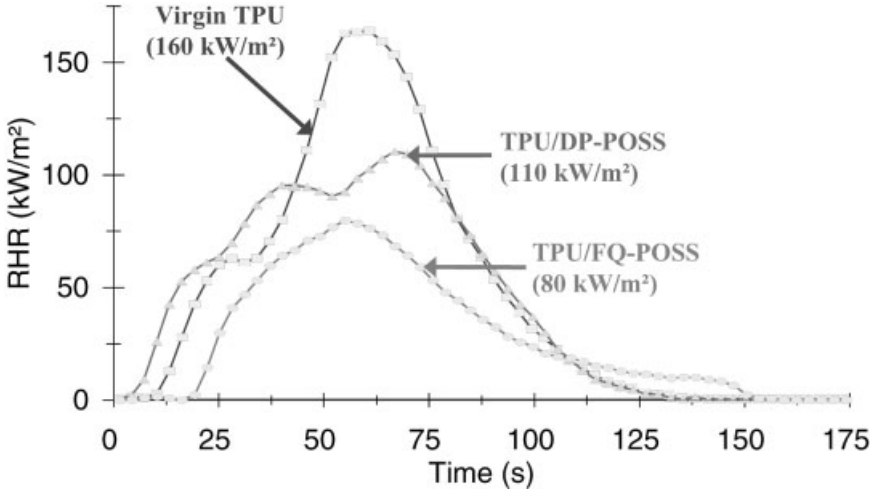

Figure 6.
Rate of heat Release (RHR) curves of TPU, TPU/DP-POSS and TPU/FQ-POSS as coating of woven PET fabrics at an external heat flux of 35 kW/m² (from [16]).

burning. The melt viscosity of the nanocomposite goes up and can prevent dripping and flowing.

In the CNT works commented above, the nanodispersion of CNT was not the main issue. According to the authors, CNTs were reasonably well dispersed but no further compatibilization was used and we suspect that some aggregates might remain. Indeed nanotubes preferentially aggregate into bundles, where adjacent tubes are held together by strong van der Waals attractions [47]. Further compatibilization can be achieved through functionalization; such as through covalently bonding organic groups directly to the CNT [48,49]. Imidazolium salts are known to be excellent cationic treatments for layered silicates (clays); they enable high temperature curing and melt processing of polymer clay nanocomposites due to their high thermal stability and excellent polymer compatibility when one of the imidazolium alkyl groups is a C-16 aliphatic chain [50]. Based on this, we have prepared well dispersed MWNT polystyrene (PS) nanocomposites via melt extrusion, using trialkylimidazolium-tetrafluoroborate (IM) compatibilized MWNTs. Quantitative TEM and laser scanning confocal microscopy (LSCM) image analysis revealed superior dispersion of the MWNTs in the presence of the

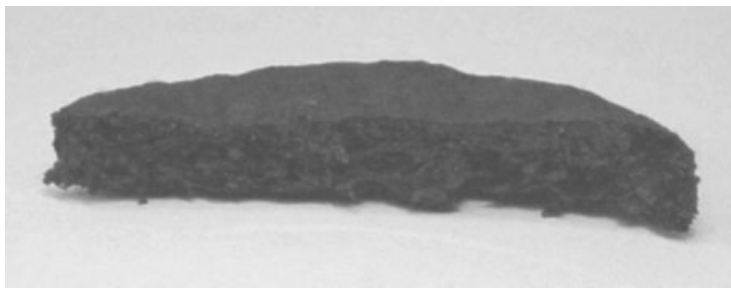

Figure 7.
The cross section of the residue of the PP/MWNT(1 wt.-%) nanocomposite after a gasification experiment at an external heat flux of 51 kW/m² (from [13]).

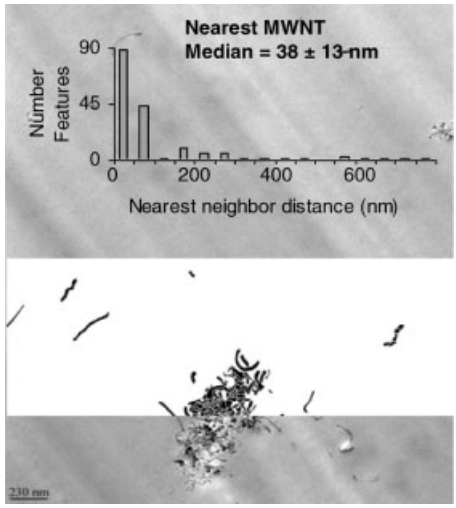

Figure 8.
TEM images of PS/MWNT (without IM) (on a part of the image the background was removed to perform image analysis).

imidazolium [51]. In particular, TEM images reveal that agglomerates (≈1 μm) of nanotubes dominate in the case of the PS/MWNT without IM (Figure 8) while well dispersed single nanotubes can be observed in the case of PS/MWNT-IM (Figure 9).

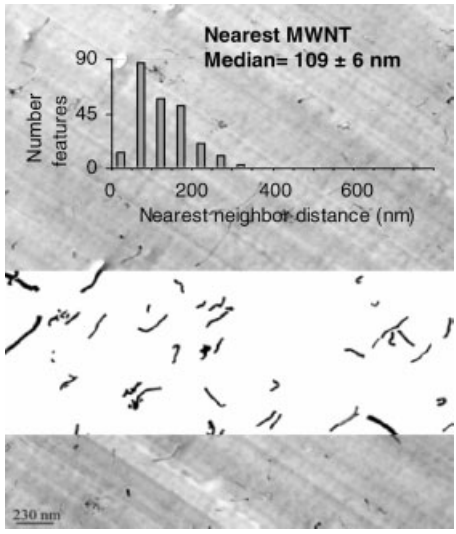

Figure 9.
TEM images of PS/MWNT-IM (on a part of the image the background was removed to perform image analysis).

The main difference between the two samples appears when the dispersion measurement is performed using image analysis techniques. When MWNT are untreated and directly incorporated in the PS poor dispersion is obtained (median nearest neighbor distance = 38 nm ± 13 nm) (Figure 8). However, the use of IM greatly improves the dispersion of MWNT in the PS matrix (median nearest neighbor distance 109 nm ± 6 nm). The theoretical nearest-neighbor distance, for a perfectly mixed sample, is 120 nm ± 15 nm for the PS/MWNT untreated and 132 nm ± 20 nm, for the PS/MWNT-IM sample (Figure 9). It appears IM acts as a compatibilizer, increasing the affinity of MWNT for the PS, and preventing the natural tendency of MWNT to aggregate.

PS nanocomposites are evaluated using a radiative gasification instrument similar to the cone calorimeter developed at NIST [52]. It is used to observe the gasification behavior and to measure mass loss rate of the samples in a nitrogen atmosphere (no burning). The unique advantages of this device are twofold: the first is that the results obtained from it are based only on the condensed phase processes due to the absence of any gas phase oxidation reactions; the second is it enables visual observation of gasification phenomena under a heat flux similar to that of a fire without any interference from a flame. Mass loss rate of the three samples recorded versus time is shown in Figure 10. Reduction of mass loss rate of PS nanocomposites is observed compared to the virgin PS but mass loss rate of PS/MWNT-IN is significantly lower than that of PS-MWNT. It indicates that the highest nanodispersion is absolutely needed to get the best performance.

General Discussion

Nanocomposites based on three different types of nanoparticles, clay, POSS and CNT were prepared and the dispersion of the particles in the nanocomposites was discussed. Their flammability properties were measured by using a cone calorimeter and a

radiative gasification apparatus in nitrogen. The results show that the reduction in heat release rate is significantly decreased compared to the virgin polymer but it appears that the nanodispersion of the filler is absolutely necessary to get the highest performance. The mechanism of protection involves in each case the formation of char layer covering the entire sample surface acting as insulative barrier and reducing volatiles escaping to the flame. The formation of such a layer not forming cracks when burning is critical to obtain low heat release rate from nanocomposites.

As we have shown above, nanocomposites tend to burn slowly and nearly completely. Although the use of a small quantity of nanoparticles evenly dispersed in polymers to form nanocomposites could be one of the alternatives to conventional flame retardants, nanocomposites need further improvements for increasing ignition delay time and for reducing total heat release. On the other hand, UL-94 test and Limiting Oxygen Index (LOI) of polymer nanocomposites are poor and those tests are very often required by the legislation. As an example, the peak of HRR of PA-6/clay nanocomposites is decreased by 63% compared to virgin PA-6 at 35 kW/m^2 while UL-94 test fails (no rating) and LOI is only 23 vol.-% [53]. Cone experiments are made in horizontal position and thus, dripping cannot occur, and the accumulation of clay at the surface can play its role of protective barrier. On the contrary, too low viscosity of the materials when heating leads to dripping when they are in vertical position (LOI and UL-94) and the protective barrier flows away from the flame and falls off. In the particular case of PA-6/MWNT, it was reported by Schartel et al. [46] that the dripping of PA-6 during UL-94 tests can make the material extinguishing while in the case of PA-6/MWNT the molten material remains in the pyrolysis zone and so, the material can burn with a larger flame and increases heat production.

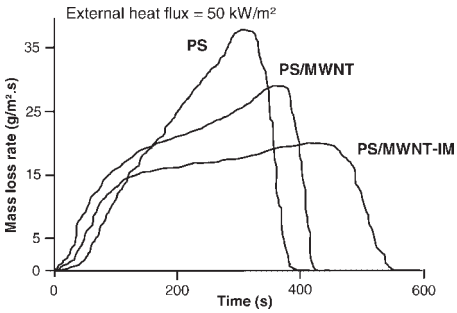

Figure 10.
Mass loss rate of the virgin PS compared to PS nanocomposites in gasification experiment at 50 kW/m^2.

The nanocomposite approach needs to be enhanced to pass specific test and/or specific fire scenarios. The combination of nanoparticles with traditional flame retardants might be the answer. In addition, it might give us the opportunity to design fire safe materials meeting specifications required by the legislation and having enhanced other properties (multifunctionality). We have developed this approach in our laboratory with the intumescent systems [54]. The concept was evaluated with the combination of ammonium polyphosphate (APP)/PA-6 and APP/PA-6/clay hybrid (hereafter called PA-6nano; PA-6 containing organomodified MMT clay nanodispersed in PA-6 and exhibiting an exfoliated structure) as intumescent systems in EVA (EVA24; EVA containing 24 wt.-% vinyl acetate). When burning the EVA24-APP/PA-6 and EVA24-APP/PA-6-nano formulations, it is observed the formation of an intumescent char which smothers the flame. One can observe that the use of PA-6-nano improves the LOI values (from 32 vol.-% without exfoliated clay to 37 vol.-% with clay at APP/PA-6 = 3 (wt/wt)). V-0 rating is achieved for $13.5 \leq \text{APP} \leq 34$ wt.% without clay and for $10 \leq \text{APP} \leq 34$ wt.% with clay (the total loadings in APP/PA-6 and APP/PA-6-nano remain equaling 40 wt.-%). This result shows that the use of PA-6-nano in the formulation allows V-0 rating to be achieved at relatively low loading in APP (10 wt.-% in comparison with 13.5 wt.-%). It is a real advantage because it permits to decrease the amount of APP in the

formulation which can lead sometimes to a blooming effect and to its migration throughout the polymer. Cone calorimeter experiment shows that HRR values of the intumescent EVA-based polymers are strongly reduced in comparison with the virgin EVA-24. It is also confirmed that the use of PA-6-nano improves flame retardancy: HRRpeak = 320 kW/m^2 with PA-6 and HRRpeak = 240 kW/m^2 with PA-6-nano. Visually a char layer is formed and intumescences after the ignition of the material. The height of the intumescent shield is about 1.5 cm compared to 0.3 cm for the non burnt material. Nevertheless after combustion, the intumescent residue of the formulation containing PA-6 nano looks less fragile than that without PA-6 nano.

Another route for making polymer with low flammability is to modify its surface laying down a thin film on the polymer using plasma assisted polymerization techniques [53]. Cold remote nitrogen plasma (CRNP) process was used to deposit thin silicon films on a PA-6 and PA-6nano substrate by reaction with 1.1.3.3-tetramethyldisiloxane monomer. LOI of PA-6 and PA-6nano treated by CRNP jump from 21 and 23 vol-% to 25 and 46 vol.-% respectively. These good results are confirmed by cone calorimeter experiment. Peaks of RHR compared to virgin PA-6 are decreased by 30% and by 60% for PA-6 and PA-6 nano treated by CNRP. This approach appears as very interesting because only one treatment of a polysiloxane coating of about 10 μm thick on polymer allows to get low flammability, but also, film deposition or hindering of additives diffusion out of the host matrix, and it can be expected that the mechanical properties of the polymer are not significantly modified.

Conclusion

Nanoparticles including organoclay, POSS and CNT can be used to make material exhibiting low heat release rate when they undergo heat. The dispersion at the nano-scale is essential to achieve the best performance. In this work, we have developed novel approaches to characterize quantitatively the nanodispersion by solid state NMR and by TEM associated with image analysis. Even if we have proven that the FR performance is directly connected to the nanodispersion versus microdispersion, work is still in progress to determine the potential impact of the morphology of the nano-mixing (e.g. intercalation vs. exfoliation).

On the other hand, low flammability of nanocomposites is only achieved in terms of HRR but they fail in terms of UL-94 and LOI. To overcome this problem, we have combined nanoparticles with traditional flame retardants (intumescents) or with plasma treatment. The nanofillers act as synergists and offer an exceptional way for making fire safe polymers meeting the requirement of the legislation. As a bonus, it should permit to take up the challenge and to succeed in designing efficient multifunctional materials. So it is our recommendation to answer our title question ''how to reach low flammability?'' to combine traditional flame retardants (in particular intumescent ones) or surface treatment to make ready to use materials passing the required legal specifications.

[1] M. Lewin, in: ''*Fire Retardancy of Polymers: The Use of Intumescence*'', M. Le Bras, G. Camino, S. Bourbigot, R. Delobel, Eds, The Royal Chemical Society, Cambridge 1998, p. 3.
[2] J. W. Gilman, T. Kashiwagi, J. D. Lichtenhan, *SAMPE J.*, **1997**, *33*, 40.
[3] J. W. Gilman, *App. Clay Sci.*, **1999**, *15*(1–2), 31–49.
[4] J. W. Gilman, T. Kashiwagi, E. P. Giannelis, E. Manias, S. Lomakin, J. D. Lichtenhan, P. Jones, in: ''*Fire Retardancy of Polymers: The Use of Intumescence*'', M. Le Bras, G. Camino, S. Bourbigot, R. Delobel, Eds, The Royal Chemical Society, Cambridge 1998, p. 223.
[5] J. Zhu, A. B. Morgan, F. J. Lamelas, C. A. Wilkie, *Chem. Mater.*, **2001**, *13*, 3774.
[6] H. Qin, Q. Su, S. Zhang, B. Zhaoa, M. Yan, *Polymer*, **2003**, *44*, 7533.
[7] S. Bourbigot, D.L. VanderHart, J.W. Gilman, S. Bellayer, H. Stretz, D.L. Paul Polymer, **2004**, *45*(22), 7627.
[8] L. Song, Y. Hu, Y. Tang, R. Zhang, Z. Chena, W. Fa, *Polym. Deg. Stab.*, **2005**, *87*, 111.

[9] A. Laachachi, E. Leroy, M. Cochez, M. Ferriol, J.M. Lopez Cuesta, *Polym. Deg. Stab.*, **2005**, *89*, 344.
[10] T. Kashiwagi, A. B. Morgan, J. M. Antonucci, M. R. VanLandingham, R. H. Harris Jr.; W. H. Awad, J. R. Shields, *J. Appl. Polym. Sci.*, **2003**, *89*(8), 2072.
[11] J. Lefebvre, M. Le Bras, S. Bourbigot, in: « *Fire Retardancy of Polymers: New Applications of Mineral Fillers* », M. Le Bras, S. Bourbigot, S. Duquesne, C. Jama, C.A. Wilkie, Eds., The Royal Society of Chemistry, Cambridge 2005, p. 42.
[12] M. Zammarano, J. W. Gilman, M. Franceschi, S. Meriani, in: ''*Proceedings of the 16th BCC Conference on Flame Retardancy*'', M. Lewin, Ed., BCC, Norwalk, CT, 2005.
[13] T. Kashiwagi, E. Grulke, J. Hilding, K. Groth, R . Harris, K. Butler, J. R. Shields, S. Kharchenko, J. Douglas, *Polymer*, **2004**, *45*, 4227.
[14] T. Kashiwagi, F. Du, K.I. Winey, K.M. Groth, J.R. Shields, S.P. Bellayer, H. Kim, J.F. Douglas, *Polymer*, **2005**, *46*, 471.
[15] E. Devaux, S. Bourbigot, A. El Achari, *J. Appl. Polym. Sci.*, **2002**, *86*, 2416.
[16] S. Bourbigot, M. Le Bras, X. Flambard, M. Rochery, E. Devaux and J. D. Lichtenhan, in: « *Fire Retardancy of Polymers: New Applications of Mineral Fillers* », M. Le Bras, S. Bourbigot, S. Duquesne, C. Jama, C.A. Wilkie, Eds., The Royal Society of Chemistry, Cambridge 2005, p. 189.
[17] P. Jash, C. A. Wilkie, *Polym. Deg. Stab.*, **2005**, *88*, 401.
[18] S. Duquesne, C. Jama, M. Le Bras, R. Delobel, P. Recourt, J. M. Gloaguen, *Comp. Sci. Tech.*, **2003**, *63*, 1141.
[19] J.W. Gilman, C.L. Jackson, A.B. Morgan, R. Harris Jr. *Chem. Mater.*, **2000**, *12*, 1866.
[20] Y. Tanga, Y. Hua, S. Wang, Z. Guia, Z. Chen, W. Fan, *Polym. Deg. Stab.*, **2002**, *78*, 555.
[21] X. Zheng, C. A. Wilkie, *Polym. Deg. Stab.*, **2003**, *82*, 441.
[22] E. Giannelis, *Adv. Mater.*, **1996**, *8*(1), 29.
[23] A. B. Morgan, J. W. Gilman, *J. Appl. Polym. Sci.*, **2003**, *87*(8), 1329.
[24] S. Bourbigot, D.L. VanderHart, J.W. Gilman, S. Bellayer, H. Stretz, D. R. Paul, *Polymer*, **2004**, *45*(22), 7627.
[25] S. Bourbigot, D.L. VanderHart, J.W. Gilman, W.H. Awad, R.D. Davis, A.B. Morgan, C.A. Wilkie, *J. Polym. Sci. B, Polym. Phys.*, **2003**, *41*(24), 3188.
[26] D. L. VanderHart, A. Asano, J.W. Gilman, *Macromolecules*, **2001**, *34*, 3819.
[27] D. L. VanderHart, A. Asano, J.W. Gilman, *Chem. Mater.*, **2001**, *13*, 3781.
[28] D. L. VanderHart, A. Asano, J.W. Gilman, *Chem. Mater.*, **2001**, *13*, 3796.
[29] J. Zhu, C. A. Wilkie, *Polymer. Inter.*, **2000**, *49*, 1158.
[30] D. W. Scott, *J. Am. Chem. Soc.*, **1946**, *68*, 356.
[31] L. Zheng, R. M. Kasi, R. J. Farris, E. B. Coughlin, *J. Polym. Sci., Part A: Polym. Chem.*, **2002**, *40*, 885.
[32] L. Zheng, R. J. Farris, E. B. Coughlin, *Macromolecules*, **2001**, *34*, 8034.
[33] H. Xu, S. W. Kuo, J. S. Lee, F. C. Chang, *Macromolecules*, **2002**, *35*, 8788.
[34] J. D. Lichtenhan, J. W. Gilman, *US Patent* 6,362,279, **2002**, assigned to US Air Force.
[35] R. A. Mantz, P.F. Jones, K.P. Chaffee, Lichtenhan, J. D. Lichtenhan, J. W. Gilman, I. M. K. Ismail, M. Burmeister, *J. Chem. Mater.*, **1996**, *8*, 1250.
[36] S. K. Gupta, J. J. Schwab, A. Lee, B.X. Fu, B.S. Hsiao, in: ''*Affordable Materials Technology – Plateform to Global Value and Performance*'', B. M. Rasmussen, L. A. Pilato, H. S. Kliger, Eds., SAMPE, Long Beach – CA 2002, *47(2)*, p. 1517.
[37] A. Fina, D. Tabuani, A. Frache, G. Camino, in: ≪ *Proceedings of FRPM'05* », B. Schartel, Ed., BAM, Berlin 2005, 12_P_23.
[38] E. Devaux, M. Rochery, S. Bourbigot, *Fire Mater.*, **2002**, *26*, 149.
[39] S. Iijima, *Nature*, **1991**, *354*, 56.
[40] M. S. P. Shaffer, A. H. Windle, *Adv. Mater.*, **1999**, *11*, 937.
[41] Z. Jin, K. P. Pramoda, G. Xu, S. H. Goh, *Chem. Phys. Lett.*, **2001**, *337*, 43.
[42] E. T. Thostenson, T.W. Chou, *J. Phys. D: Appl. Phys.*, **2002**, *35*, L77.
[43] Y. Bin, M. Kitanaka, D. Zhu, M. Matsuo, *Macromolecules*, **2003**, *36*, 6213.
[44] T. Kashiwagi, E. Grulke, J. Hilding, R. H. Harris Jr., W. H. Awad, J. Douglas, *Macromol. Rapid Commun.*, **2002**, *23*, 761.
[45] G. Beyer, *Fire Mater.*, **2002**, *26*, 291.
[46] B. Schartel, P. Pötschke, U. Knoll, M. Abdel-Goad, *Eur. Polym. J.*, **2005**, *41*, 1061.
[47] A. Thess, R. Lee, P. Nikolaev, H. Dai, P. Petit, J. Robert, C. Xu, Y-H. Lee, S-G. Kim, A. G. Rinzler, D. T. Colbert, G. E. Scuseria, D. Tomanek, J. E. Fischer, R. E. Smalley, *Science*, **1996**, *273*, 483.
[48] A. Hirsch, *Angew. Int. Ed.*, **2002**, *41*, 11.
[49] S. Cui, R. Canet, A. Derre, M. Couzi, P. Delhaes, *Carbon*, **2003**, *41*, 797.
[50] J. W. Gilman, W. H. Awad, R. D. Davis, J. Shields. R. H. Harris Jr., C. Davis, A. B. Morgan, T. E. Sutto, J. Callahan, H. C. Trulove, H. DeLong, *Chem. Mater.*, **2002**, *14*, 3776.
[51] S. Bellayer, J. W. Gilman, N. Eidelmen, S. Bourbigot, X. Flambard, D. M. Fox, H. C. DeLong, P. C. Trulove, *Adv. Funct. Mater.*, **2005**, *15*, 910.
[52] P.J. Austin, R.R. Buch, T. Kashiwagi, *Fire Mater.*, **1998**, *22*, 221.
[53] C. Jama, A. Quédé, P. Goudmand, O. Dessaux, M. Le Bras, R. Delobel, S. Bourbigot, J. W. Gilman and T. Kashiwagi, in: « *Fire and Polymers: Materials and solutions for hazard prevention* », G. L. Nelson, C. A. Wilkie, Eds, American Chemical Society (ACS), Washington DC 2001, p. 200.
[54] S. Bourbigot, M. Le Bras, S. Duquesne, M. Rochery, *Macromol. Sci. Eng.*, **2004**, 289(6), 499.

